Human Molecular Genetics, 2024, Vol. 33, 15, 1300–1314
https://doi.org/10.1093/hmg/ddae072
Advance access publication date 27 April 2024
Original Article

An integrative miRNA-mRNA expression analysis identifies miRNA signatures associated with *SOD1* and *TARDBP* patient-derived motor neurons

Banaja P. Dash[1], Axel Freischmidt[2], Jochen H. Weishaupt[3], Andreas Hermann[1,4,5,*]

[1]Translational Neurodegeneration Section "Albrecht Kossel", Department of Neurology, University Medical Center Rostock, Gehlsheimer Str. 20, Rostock 18147, Germany
[2]Department of Neurology, Ulm University, Albert-Einstein-Allee 11, Ulm 89081, Germany
[3]Division of Neurodegeneration, Department of Neurology, Mannheim Center for Translational Neurosciences, Medical Faculty Mannheim, Heidelberg University, Theodor-Kutzer-Ufer 1-3, Mannheim 68167, Germany
[4]Center for Transdisciplinary Neurosciences Rostock, University Medical Center Rostock, Gehlsheimer Str. 20, Rostock 18147, Germany
[5]Deutsches Zentrum für Neurodegenerative Erkrankungen (DZNE) Rostock/Greifswald, Gehlsheimer Str. 20, Rostock 18147, Germany
*Corresponding author. Translational Neurodegeneration Section "Albrecht Kossel", Department of Neurology, University Medical Center Rostock, 18147 Rostock, Germany. E-mail: andreas.hermann@med.uni-rostock.de

Abstract

MicroRNAs (miRNAs) are a subset of small non-coding single-stranded RNA molecules involved in the regulation of post-transcriptional gene expression of a variety of transcript targets. Therefore altered miRNA expression may result in the dysregulation of key genes and biological pathways that has been reported with the onset and progression of neurodegenerative diseases, such as Amyotrophic lateral sclerosis (ALS). ALS is marked by a progressive degeneration of motor neurons (MNs) present in the spinal cord, brain stem and motor cortex. Although the pathomechanism underlying molecular interactions of ALS remains poorly understood, alterations in RNA metabolism, including dysregulation of miRNA expression in familial as well as sporadic forms are still scarcely studied. In this study, we performed combined transcriptomic data and miRNA profiling in MN samples of the same samples of iPSC-derived MNs from *SOD1*- and *TARDBP* (TDP-43 protein)-mutant-ALS patients and healthy controls. We report a global upregulation of mature miRNAs, and suggest that differentially expressed (DE) miRNAs have a significant impact on mRNA-level in SOD1-, but not in TARDBP-linked ALS. Furthermore, in SOD1-ALS we identified dysregulated miRNAs such as miR-124-3p, miR-19b-3p and miR-218 and their potential targets previously implicated in important functional process and pathogenic pathways underlying ALS. These miRNAs may play key roles in the neuronal development and cell survival related functions in SOD1-ALS. Altogether, we provide evidence of miRNA regulated genes expression mainly in SOD1 rather than TDP43-ALS.

Received: January 28, 2024. **Revised:** March 27, 2024

Graphical Abstract

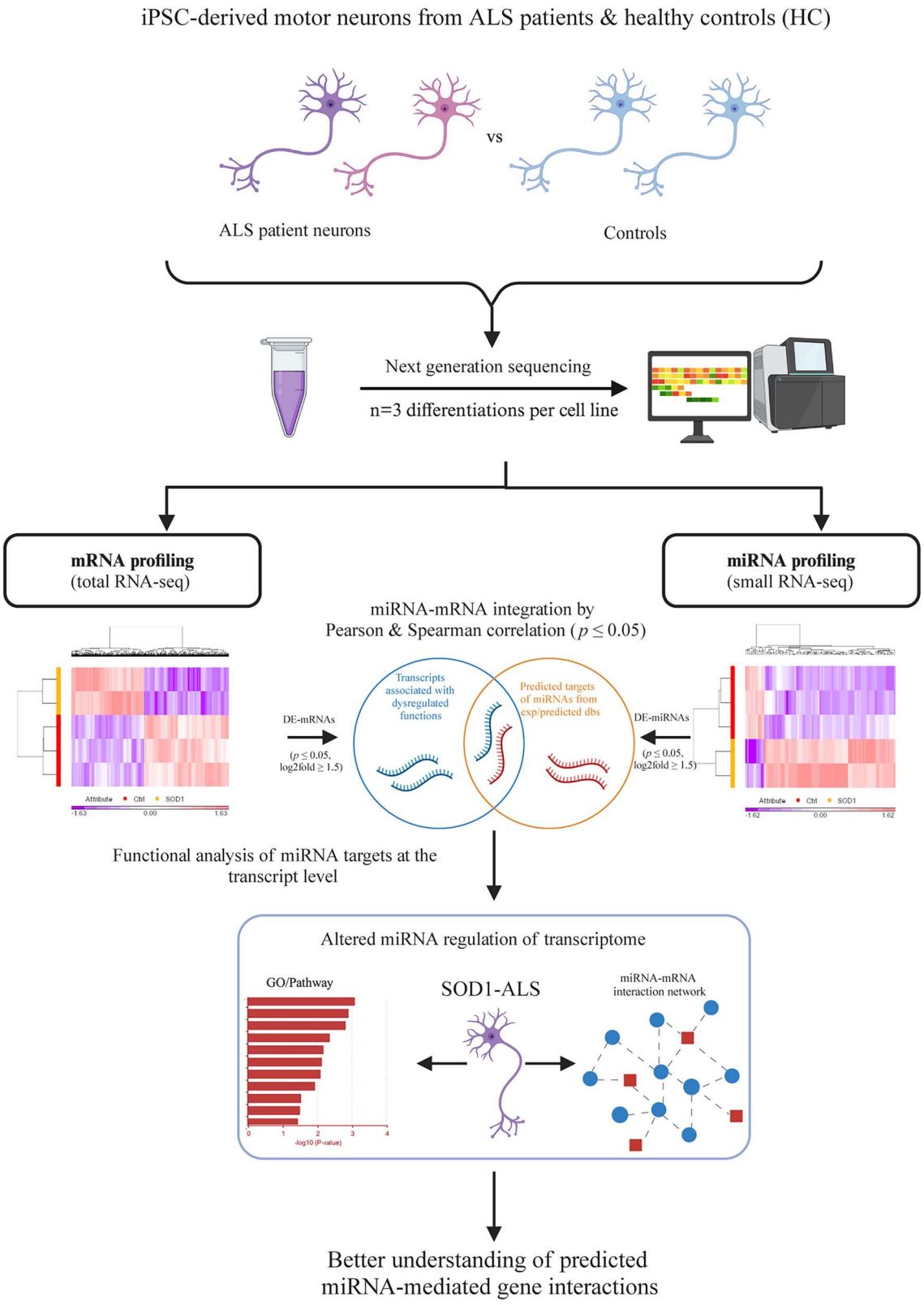

Keywords: amyotrophic lateral sclerosis; human induced pluripotent stem cells; motor neurons; RNA sequencing; microRNA; differentially expressed

Introduction

Amyotrophic lateral sclerosis (ALS) is a progressive and irreversible neurodegenerative disease characterized by predominant loss of motor neurons in the motor cortex, brain stem and spinal cord. The majority of ALS cases are sporadic (sALS), while the remaining 5-10% are familial (fALS). To date, approximately 40 relevant genes associated with ALS pathogenesis have been identified; among these gene mutations to chromosome 9 open reading frame 72 (*C9orf72*), Cu/Zn superoxide dismutase 1 (*SOD1*), TAR-DNA-binding protein 43 (*TARDBP*) and fused in sarcoma (*FUS*) are the most common and have the highest penetrance [1–3]. These causative genes encode proteins with different functions, which are associated with protein aggregation, defects in stress response, aberrant RNA metabolism, transcription, epigentic changes and microRNA (miRNA) processing [4, 5]. Despite extensive research, the underlying pathomechanisms in general but also those which are likely causing motor neuron degeneration and cell death of these gene mutations remain unknown.

Presently, alteration in all aspects of RNA biology is considered to be one of the most important events and can lead to neural dysfunction and neurodegeneration, especially for those genes known to be RNA binding proteins such as FUS or TDP43. Despite lacking RNA-binding motifs mutant SOD1 was reported to trigger dysfunction across miRNA biogenesis and mRNA stabilization and support [6–9], thus suggesting its potential role in regulating RNA metabolism similar to other RNA-binding proteins such as FUS and TDP-43. miRNAs are a class of highly conserved, small (∼20–23 nucleotides in length) endogenous non-coding RNAs that regulate more than 60% of human protein coding genes, indicating their important function within physiological and pathological cellular processes [10, 11]. They negatively regulate gene expression post-transcriptionally by guiding the RNA induced silencing complex (RISC) to the 3′-untranslated region (UTR) of specific mRNAs resulting in degradation, deadenylation or translational repression of the target mRNAs. [12–14]. In addition, a single miRNA may target several hundred mRNAs, while a single mRNA may be targeted by several miRNAs. [15, 16]. Studies including ALS mouse models and human tissues have reported that miRNA dysregulation is involved in various pathological pathways related to ALS [17–20]. Moreover, mutations in *SOD1* and *TARDBP* cause aberrant expression of miRNAs, perhaps representing two different disease pathways to ALS, which could be used as a valuable tool to detect changes during disease onset and progression, and develop therapeutic biomarkers or treatments for ALS [21–23].

In recent years, the use and integration of high-throughput RNA-based omics approaches, including small and long RNA sequencing have dramatically improved our understanding on which pathways might lead to MN degeneration implicated in ALS pathobiology. Several studies showed differential expression of either mRNAs or miRNAs in MNs of *in vitro* SOD1 and TARDBP ALS models and to the best of our knowledge, very few studies have paid attention to the important roles of miRNA and mRNA expression patterns by combining transcriptomic data and miRNA profiling in MN samples of the same ALS patient [24–27]. Moreover, considering both types of expression data, miRNAs and mRNAs from the same patient lines might help to identify regulatory networks of functional miRNA-mRNA interactions and to understand the molecular basis of their action involved in ALS disease. Two papers from our group contributed to the global PPI network [28] and transcription factor analysis to generate interactome maps of iPSC-derived motor neurons from ALS subtypes (SOD1 and TARDBP) using microarray and RNA-Seq profiling studies, identifying gene expression as a common pathomechanism in both corroborating that many genes in TARDBP-ALS were associated with RNA transcription at one level, whereas genes identified in SOD1-ALS were connected to protein translation at another level [29, 30]. We now wanted to analyse how much of these effects might derive from miRNA-mediated regulation of mRNA expression.

For this, we performed an extensive transcriptomic investigation (high-throughput-next generation sequencing, HT-NGS) to study the contribution of miRNA dysregulation in ALS pathogenesis using *SOD1*- and TARDBP-iPSC derived MNs and control subjects. We identified several key miRNAs and their predicted mRNA targets in motor neurons, and further explained biologically relevant pathways and gene functions affected by the miRNA-mRNA target pairs to gain insight into ALS disease. Most importantly, our results revealed striking impact of a global upregulation of miRNAs expression that target gene expression in SOD1- but not TARDBP-ALS patients respect to controls.

Results

RNA-Seq profiling and identification of differentially expressed miRNAs in SOD1- and TARDBP-ALS

To gain insight into how altered miRNAs affect target genes/pathways in the dysregulation of mRNAs previously identified in MNs [29], we performed miRNA- and RNA-sequencing on the same RNA samples from SOD1- (R115G and homozygous D90A) and TARDBP-ALS (S393L and G294V) patients and three healthy and unrelated controls and screened for negatively correlated miRNA-mRNA pairs. A detailed outline of the work flow is summarized in Fig. 1. The cells lines and their in depth characterization was reported previously [29, 31, 32]. miRNA profiling identified a total of 95 mature differentially expressed (DE) miRNAs in SOD1-ALS, among which 83 miRNAs were upregulated and 12 miRNAs were downregulated. In TARDBP-ALS, we ended up with 42 DE-miRNAs and of these miRNAs, 18 were upregulated and 24 were downregulated in patients compared with healthy controls (Fig. 2). Focusing on our previously published GEO dataset of the same eight samples (GSE210969), RNA profiling identified 1448 DE-mRNAs in SOD1-ALS, with 668 upregulated and 780 downregulated genes and 1160 DE-mRNAs with 626 upregulated and 534 downregulated genes were expressed in TARDBP-ALS compared to their controls [29]. The cut-off criteria were set at P-value ≤ 0.05 and $|\log2FC| \geq 1.5$ (FC, fold change) for identifying DE-mRNAs and DE-miRNAs. All differential expression analysis results are provided in Supplementary Material, Table S1.

Integrated target prediction analysis of differentially expressed miRNAs

To avoid false prediction and further improve the reliability/specificity of our subsequent results of the target genes of the screened DE-miRNAs, we applied an integrated approach of validated and predicted interaction data extracted from five different databases containing experimentally validated and computationally predicted miRNA-target interactions for the SOD1- and TARDBP-ALS patients and healthy controls (detailed in the methods section). To identify mRNAs putatively regulated by specific miRNAs, we performed an inverse correlation analysis at the probe level between the expression of a specific miRNA and the expression levels of all the predicted mRNA targets within the differentially expressed mRNAs of the miRNAs by above databases (Fig. 3A).

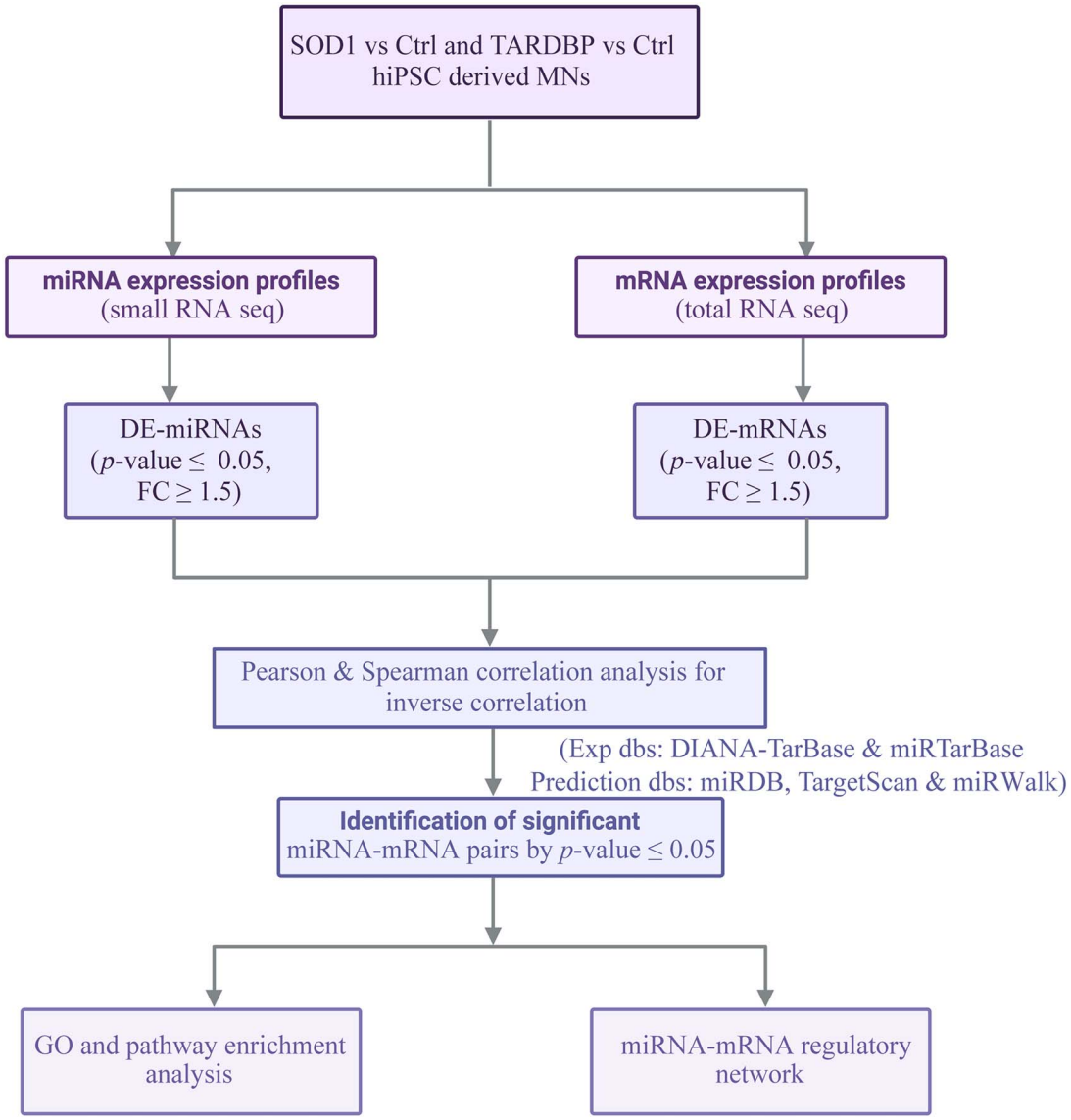

Figure 1. The workflow of the study. The small RNA data were generated in the current study and total RNA sequencing data were obtained from a previously published study [29]. Gene expression profiles of miRNAs and mRNAs were computed as outlined in the figure according to the $|\log2FC| \geq 1.5$ and *P*-value ≤ 0.05. We performed an integrated analysis of miRNA and mRNA expression data based on the Pearson and Spearman correlation analysis and miRNA target prediction datasets were identified using five different databases; TargetScan, miRDB, miRWalk, miRTarBase and TarBase. Finally, downstream analysis of gene ontology (GO), and pathway annotation was performed using EnrichR tool. regulatory network was generated using Cytoscape v3.10.1 software. Abbreviations: MN, motor neurons; DE-mRNA, differentially expressed mRNAs; DE-miRNA, differentially expressed miRNAs; GO, gene ontology; KEGG, Kyoto Encyclopedia of Genes and Genomes; dbs, databases; NGS, next generation sequencing.

Pearson and Spearman correlation analysis was performed to examine the DE-miRNAs and DE-mRNAs and the test results are summarized in Supplementary Material, Tables S2 and S3. Since miRNAs act as negative regulators, upregulated miRNAs would result in downregulated target mRNAs in the same corresponding samples, and vice versa. This combination of correlations and target predictions analysis identified miRNA-mRNA pairs in SOD1-ALS and TARDBP-ALS. To our surprise, only in case of SOD1-ALS, but not TARDBP-ALS, we found a significant enrichment (Fisher's exact test *P*-value = < 0.0001; Fig. 3B) yielding 230 downregulated targeted mRNAs associated with 62 upregulated miRNAs (Supplementary Material, Fig. S1A–C and Table S1) and emplyed for further analysis. In contrast, 9 downregulated miRNAs were screened targeting 9 upregulated mRNAs (Fisher's exact test *P*-value = 0.5344) (Fig. 3C).

Similarly in TARDBP-ALS, predicted miRNA–mRNA pairs (Fig. S2A) contained 10 upregulated miRNAs targeting 15 downregulated mRNAs (Fisher's exact test *P*-value = 0.2393) (Fig. S2B), and 18 downregulated miRNAs targeting 33 upregulated mRNAs (Fisher's exact test *P*-value = 0.3814), suggesting predicted mRNA targets of dysregulated miRNAs were not greatly enriched and/or anticorrelated in case of TARDBP mutants (*P*-value ≥ 0.05) (Fig. S2C).

We next asked, which miRNA-target gene interactions are central across all datasets (i.e, of the common 62 miRNAs-230 downregulated targets) in SOD1-ALS. Thus, we decided to analyze further a set of four top occurring miRNAs (miR-124-3p, miR-19b-3p, miR-218 and miR-145-5p), that regulate the expression of at least three target genes (cutoff criteria, DE-miRNAs ≥ 3 DE-mRNAs = 23 targets, see methods section) simultaneously

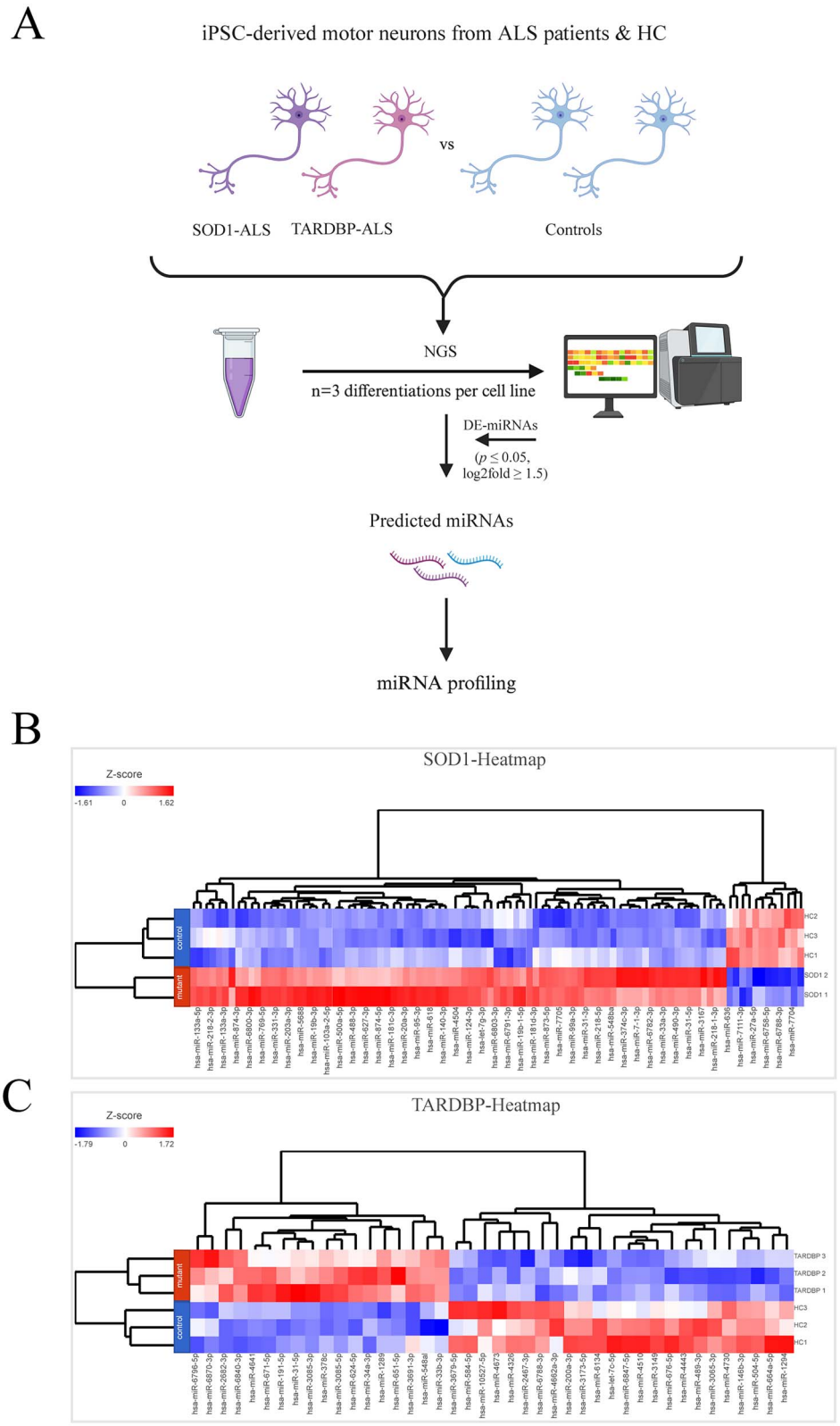

Figure 2. Identification of differentially expressed miRNAs. A total of 95 DE-miRNAs (83 up and 12 down) in SOD1 and 42 DE-miRNAs in TARDBP (18 up and 24 down) were identified in ALS and healthy controls (HC). (A) Schematic diagram showing differential expression of miRNAs using iPSC-derived MNs to address perturbed expression of gene regulations in ALS patients and HC. The neurons and miRNAs are colored accordingly. (B) The heatmap showing the differential expression of significant (*P*-value ≤ 0.05) miRNAs based on ≥ 1.5-fold changes in *SOD1* mutant (SOD1 1, $SOD1^{D90A}$; SOD1 2, $SOD1^{R115G}$) and HC. (C) The heatmap exhibited significant (*P*-value ≤ 0.05) differentially expressed miRNAs based on ≥ 1.5-fold changes in *TARDBP* mutant (TARDBP 1 and TARDBP 2 (2 clones from one patient), $TARDBP^{G294V}$; TARDBP 3, $TARDBP^{S393L}$) and HC. Heatmaps were generated in *Partek*™ *Flow*™ software, v11.0 using normalized (separate Z-score calculated per gene) expression values across all samples (ALS patients and HC) in units of RPKM (ANOVA test). Each row in the heatmap represents a sample, and each column represents a miRNA and the color scale at the left of the heatmap represents the Z-score ranging from blue (low expression) to red (high expression), respectively. Abbreviations: DE, differentially expressed; HC, healthy controls; RPKM, Reads Per Kilobase per Million mapped reads; ANOVA, analysis of variance; NGS, next generation sequencing.

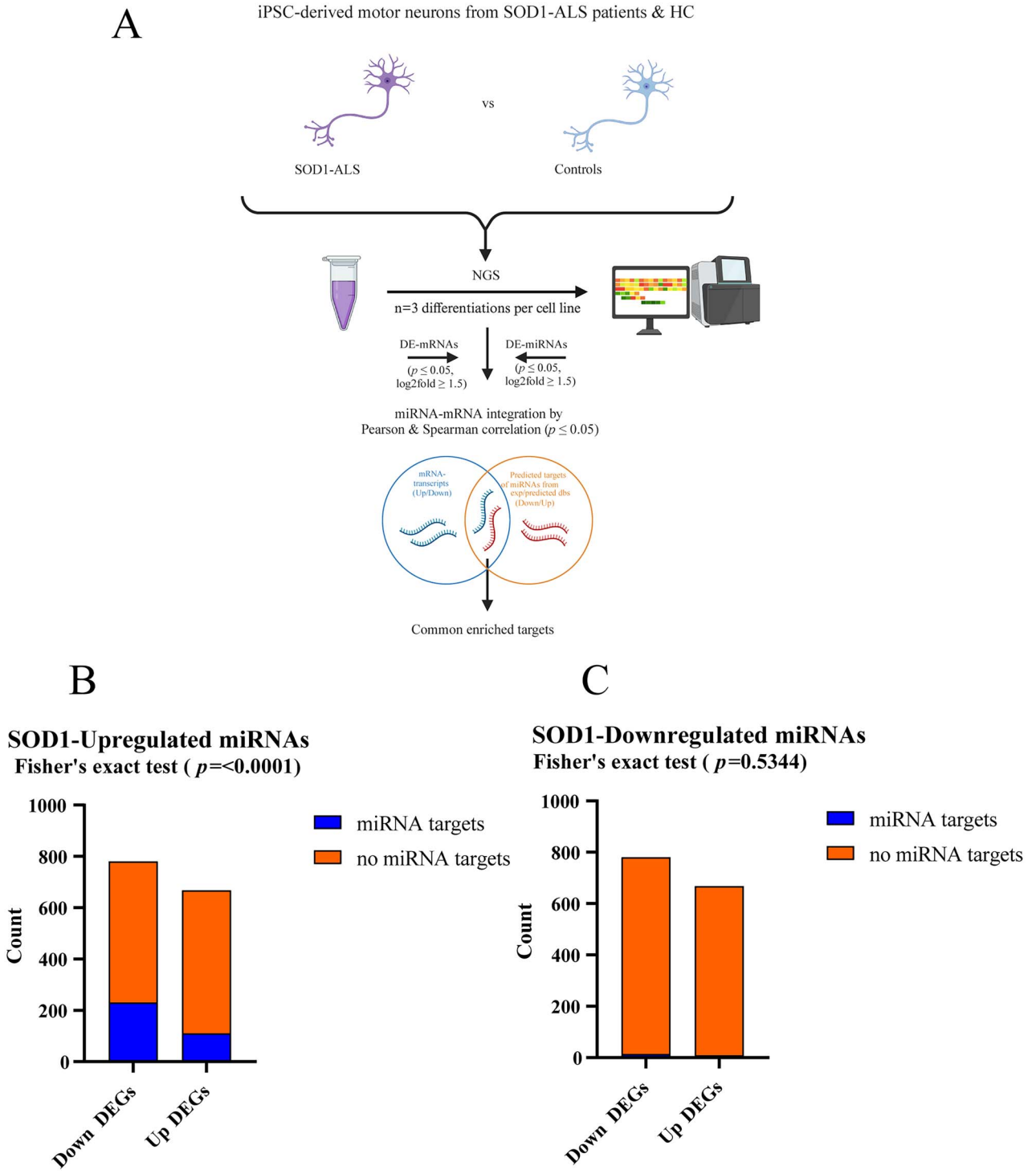

Figure 3. Target enrichment analysis in SOD1-ALS. (A) Schematic summarizing differential expression of miRNAs/mRNAs and target enrichment analysis using different databases. Enriched targets were used for further analysis. (B) Target enrichment graph of upregulated miRNAs displaying significant enrichment of its 230 downregulated targets (experiment ∩ predicted databases, Fisher's exact test *P*-value = < 0.0001). (C) Target enrichment graph of downregulated miRNAs (experiment ∩ predicted databases, Fisher's exact test *P*-value = 0.5344) showing no enrichment of its upregulated mRNA targets. For the enrichment analysis, predicted and validated miRNA-mRNA pairs were extracted from the five different databases and only the significant enriched miRNA-mRNA pairs predicted by these databases were retained. enrichment graphs were analyzed in GraphPad prism v9.4.1 (*P*-value ≤ 0.05). Abbreviations: DE, differentially expressed; NGS, next generation sequencing; dbs, databases.

collected from all five distinct databases. We believe that these 4 candidate miRNAs along with their 23 potential targets may perform an important role in the regulation of gene expression in SOD1-ALS (Table 2). Since there is a considerable difference in the number of occurrence counts list from the list of putative miRNA target genes between the different databases/programs used, this extended the analysis to additional molecular players, possibly exploring some overlapping miRNAs/mRNAs that may be linked to SOD-ALS (Supplementary Material, Fig. S4).

Functional and pathway enrichment analysis of the predicted target genes

To determine the functional consequence of miRNA mediated mRNA regulation identified by the miRNA-mRNA inverse correlation approach, gene ontology (GO) and pathway enrichment analyses of above 23 target genes were performed using the EnrichR enrichment tool (P-value ≤ 0.05). In SOD1 mutant cells, the results indicated that the target mRNAs were predominantly enriched in biological processes (BP) associated with regulation of nuclear-transcribed mRNA poly(A) tail shortening and mRNA-related catabolic processes (Fig. 4A). In terms of molecular function (MF), the mRNA targets were mostly enriched in transporter activity functions. For cellular component (CC) category, the target genes were mainly enriched in serine/threonine protein kinase complex (Supplementary Material, Fig. S3A and B). In addition, Reactome and KEGG pathway enrichment analysis revealed that these target genes were primarily mapped into transport of salts/acids/ions/amines, p53-signaling pathway and activation of hemeobox (HOX) genes during differentiation (Fig. 4B and C). Further details of significantly implicated pathways and GO terms are reported in Supplementary Material, Table S4).

miRNA-target regulatory network analysis

The miRNA-mRNA regulatory network containing top four most frequent miRNAs (high degree) and their matched 23 mRNA targets obtained from experimental and predicted databases is given in (Fig. 5A and B). Of these, top miR-124-3p, miR-19b-3p, miR-218, and miR-145-5p indicate a possible direct suppressive regulation with a high degree of connectivity between miRNAs and their target mRNAs. These downregulated mRNA-targets were mainly associated with nervous sytem related functions, respectively. Taken together, we showed that the miRNA-mRNA network generated using these top regulated miRNAs can indeed be partly representative of the transcriptome changes, which implies that these miRNAs have set up the important transcription regulatory network in the investigated samples.

Discussion

ALS is a multifactorial disease in which several genes have been implicated in RNA biology including TARDBP, FUS and others, but the actual pathophysiological changes are determined by multiple genomic and proteomic alterations taking place in a complex biological network. Thus, global gene expression, which involves studying expression changes in both coding genes as well as non-coding genes regulating neuronal function is an attractive strategy to identify the potential molecular pathological networks involved in ALS. Several gene expression studies have investigated biological pathways such as neuronal function, differentiation, development, and progression of diseases [33, 34], exploring their potential function has recently gathered increased interest in MN development and in the etiology of ALS. Indeed, plenty of DE-miRNAs have been identified in blood, muscle tissue, cerebrospinal fluid (CSF), spinal cord, brain, and iPSCs of ALS patients differing from that of healthy controls [20, 25, 35–39]. Using mRNA expression analysis, we recently identified gene expression as a common pathomechanism in both iPSC-derived MNs from SOD1- and TARDBP-ALS patients [29, 30]. Of note, while many genes in TARDBP-ALS were associated with RNA transcription, genes identified in SOD1-ALS were connected to protein translation [29]. As an attempt to see whether SOD1-ALS disease phenotypes could be differentiated by miRNAs expression and target regulation, we performed a HT-NGS method followed by an integrated bioinformatics analysis of both miRNAs and mRNAs samples from the same subjects (ALS patients and healthy controls). The additional noteworthy finding is that only in case of SOD, but not TARDBP-ALS, we found a significant enrichment of predicted target datasets for commonly upregulated miRNAs, whereas no significant differences were found in the target enrichment of downregulated miRNAs. In contrast, no significant miRNA-mRNA interactions was observed in TARDBP, indicating that either TARDBP mutations cause dramatic changes to the transcriptome that may dominate/mask miRNA-mRNA relations, or TARDBP is required for miRNA function. We believe it might be explained by the RNA-binding behavior/mechanism of TARDBP which may have a large impact on the entire repertoire of mRNA transcriptional regulation. Our data are coherent with previous studies, although not strictly an RNA-binding protein, mutant SOD1 emerges with similar capabilities like in TARDBP in inducing dysfunction across miRNA-processing and gene expression and mRNA stability in ALS disease [7, 8, 40].

A prominent finding of our study is that we identified altered expression of both miR-124-3p and miR-218 among the detected negatively regulated miRNA-mRNA interaction pairs, which are the most investigated miRNAs in the field of ALS [41, 42] and have been reported in other neurodegenerative diseases as well [43]. Specifically, miR-124 represents one of the most abundant miRNAs in many neuronal subtypes and acts an important neurodevelopmental regulator in promoting neurogenesis and maintaining neuronal cell identity as well as synaptic plasticity [44–46]. In addition, the increased levels of miR-124 was shown to exert beneficial or pathogenic effects among different studies depending on the disease experimental models and the type of neurons/cell type identity [41]. In mutant $SOD1^{G93A}$ mouse model increased levels of miR-124 were reported in spinal cord and brainstem at both pre-symptomatic and symptomatic stages of the disease [47, 48], suggesting that altered expression of neural (miR-124, miR-9) and cell cycle-related miRNAs (miR-19a, miR-19b) in the brain regions might contribute to ALS pathogenesis [49]. On the other hand, its elevated levels were highlighted to be protective in spinal cord injury [50]. Given the presence of miR-124 and miR-19b increased levels in both tissues (brain and spinal cord) of ALS mouse model [41, 47, 49, 51] and circulating fluids (blood, CSF, CSF-spinal cord/nervous tissue overlap) of ALS patients [51–55], we also detected a significantly elevated expression of miR-124-3p and miR-19b-3p in iPSC-derived MNs from SOD1-ALS samples compared to their healthy controls. Through our enrichment analysis, we found that miR-124-3p and miR-19b-3p might downregulate p53 signaling/cell cycle regulation pathways, supporting miRNAs putative role in either survival mechanisms or in pathogenicity/neuronal death [56]. Among the most frequent target genes of miR-124-3p in the present study was the cyclin D-kinase 6 dependent gene (CDK6) involved in p53 activity regulation pathway from our pathway analysis. It was already shown that miR-124 was highly expressed in cells at G0/G1 phase [57], which resulted in the downregulation of CDK6, thus regulating cell cycle progression from G0/G1 [58]. Previous studies have suggested that a failure of cell cycle regulation could lead to the post-mitotic MNs attempting to re-enter the cell cycle, leading to cell death associated with the neurodegeneration onset. That would also explain the increased expression of miR-124-3p in mutated MNs and consequent downregulation of CDK6 may contribute to prevent the re-entry in cell cycle at early disease stages.

Of particular interest is the differential expression of miR-218, a motor neuron-enriched miRNA, which also appears to be

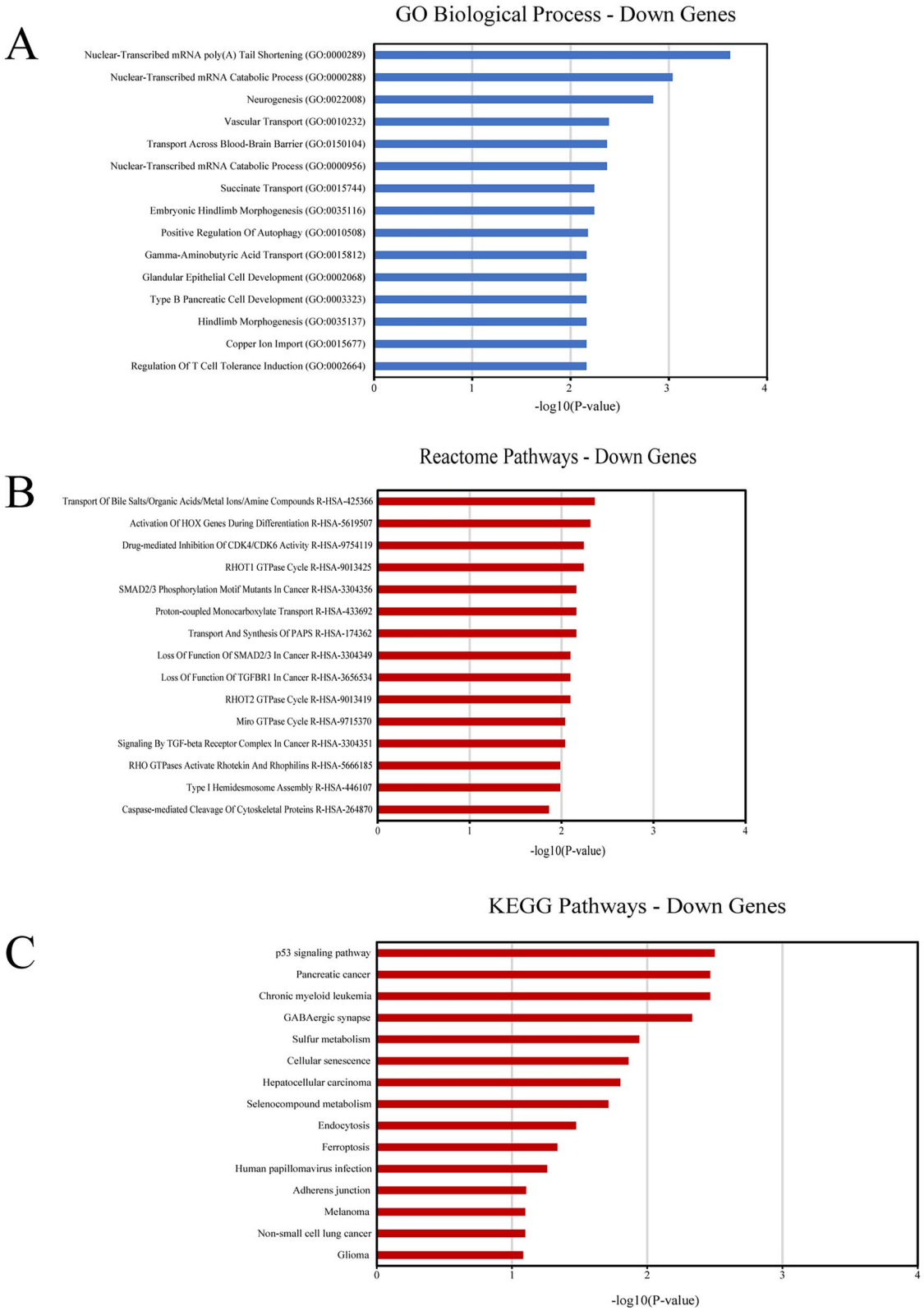

Figure 4. Functional enrichment analysis of miRNA-target genes in SOD1-ALS. (A) Bar graph of top 15 enriched GO terms (BP) of DE-miRNAs-associated downregulated genes. (B) Bar graph of top 15 enriched pathway (Reactome) terms across lists of input downregulated genes. (C) Bar graph of top 15 enriched pathway (KEGG) terms across lists of input downregulated genes. The enrichment analysis was performed by EnrichR and P-value represents the importance of enrichment. Y-axis represents the GO/pathway term, and the X-axis represents the enrichment significance (−log10 (P-value)), respectively. Abbreviations: GO, gene ontology; BP, biological process; DE, differentially expressed.

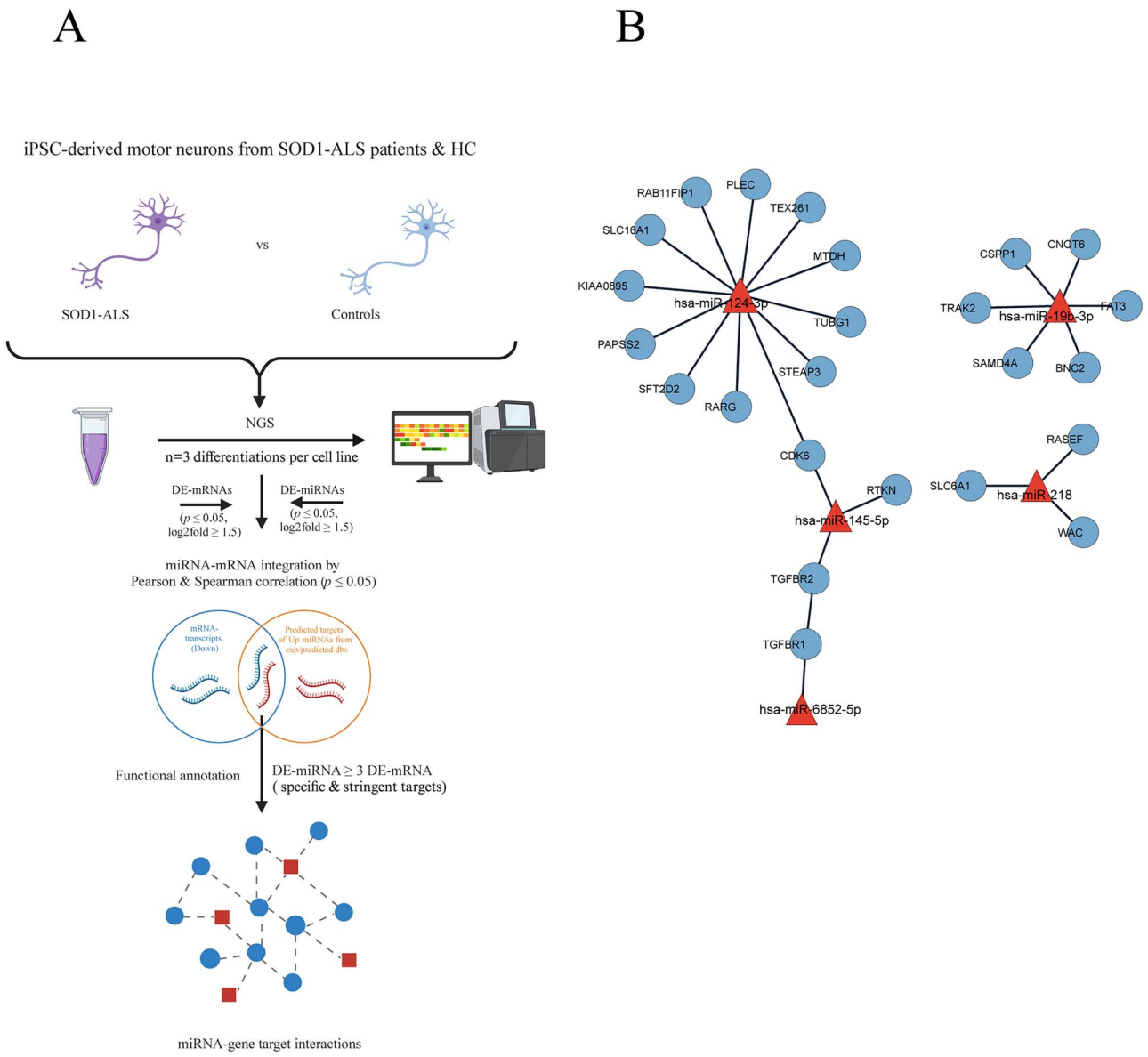

Figure 5. Network of high-confidence occurring miRNA-mRNA interactions and functional connections among target genes in SOD1-ALS. (A) Schematic overview of identifying miRNA-mRNA regulatory networks involved in ALS-dysregulated processes/pathways. (B) Network of the top occurring miRNA-mRNA interactions based on upregulated miRNAs and their possible target mRNAs (at least three target genes), and their inside regulations in our dataset (negatively correlated -$P \leq 0.05$- and predicted simultaneously in five different databases). In the network, miR-6852-5p is also highlighted due to its relevant interactions with the target involved in TGF-beta pathway. Round ellipses represent mRNA (blue color), while triangles represent miRNA (red color). The miRNA-mRNA pairs were constructed using the miRNAs with high degree of connectivity within the network (topological parameters) and the generated networks were visualized using Cytoscape v3.10.1 software. Abbreviations: DE, differentially expressed; NGS, next generation sequencing; dbs, databases.

upregulated in our iPSC-derived MNs from SOD1-ALS patients compared to healthy controls. Moreover, this MN-enriched miRNA had the increased expression in adult mouse MNs (SOD1^{G93A}) compared with all other spinal cord neurons and was detected mainly in the ChAT^{+} MNs in the anterior horns of the spinal cord but not in other cell types [59]. Previous studies in both chick neural tube and mouse embryonic stem cells have reported that the expression of miR-218 (*miR-218-1* and *miR-218-2*) was significantly upregulated by the Isl1–Lhx3 complex, which drives motor neuron cell fate specification in developing and adult MNs, suggesting that miR-218 plays an important role in mature MN differentiation [60]. In addition, the authors used an unbiased robust RISC-trap screen approach to identify direct miR-218 target mRNAs, such as solute carrier family 6 (neurotransmitter transporter, GABA), member 1 gene (SLC6A1) as well as other spinal interneurons/progenitor targets, suggesting a potential function for miR-218 in regulating neurite morphogenesis and synapse development while suppressing this non-MN gene during MN differentiation [60]. In agreement with the above finding [60], we also identified SLC6A1 target and related transport of small molecules/SLC mediated transport pathways being downregulated in SOD1-ALS MNs. On the other hand, to our knowledge, miR-145-5p is not associated with ALS, however, in our study we showed miR-145-5p and miR-6852-5p could be involved in the selective decrease of target genes like TGFBR1 and TGFBR2, key mediator of transforming growth factor beta signaling pathway (TGF-beta) involved in essential cellular and physiological processes, that are placed in specific nodes of our

molecular networks. Dysregulation of the TGF-beta pathway has been well reported in ALS affecting MNs [61]. Especially, in a meta-analysis of publicly available transcriptomic datasets revealed that TGF-beta/SMAD targets were downregulated in iPSC-derived MNs from patients with mutant $SOD1^{A272C}$ and control subjects [62], fitting to our results obtained. During development and under neuronal stress/injuries, TGF-beta1 levels rapidly increased promoting the expression of multiple genes involved in neuroprotection mechanism to protect MNs against neuronal damage [63]. Along the same lines, a recent study has confirmed that high levels of TGF-beta1/beta3 in the serum might display a compensatory effect to counteract the pronounced systemic immune response typical of the late stage of the disease, suggesting the negative correlation between TGF-beta levels and ALS patients [64]. On the other hand at the level of the central nervous system (CNS)/skeletal muscle, functional *in vitro* studies demonstrated reduced levels of TGF-beta1 in the spinal cord and increased selectively in the skeletal muscle of pre-symptomatic mutant SOD1 mice, indicating a lack of the TGFB neuroprotective/compensatory responses in the early stages of the disease (presumbly due to glutamate excitotoxicity), whereas at the symptomatic stage TGFB levels are largely increased both in the mouse spinal cord and muscle, as well as in the muscle biopsies of sALS patients [65], indicating probable development of reactive astrogliosis in the neurotoxic environment, thus exacerbating the disease progression [65]. Similarly, TGF-beta2 levels are increased in human and mouse spinal cord ALS samples, indicating a higher TGF-beta2 immunoreactivity in the motor nerve terminals [65, 66]. In conformity, we hypothesize that the TGF-beta pathway may be considered critical for SOD1-ALS etiology/progression and downregulation of both target genes associated with TGF-beta network might indicate a lack of the protective response to counteract motor neuronal damage during the early stages of the disease. Overall, we reported predicted effects of miR-124-3p, miR-19b-3p, miR-218 and miR-145-5p targeting the identified genes and critical pathways involved in a wide range of cellular functions by *in silico* methods, indicating their potential involvement in the complex SOD1-ALS pathophysiology and warrantes further investigations.

Limiations of our study include the small sample size. Furthermore the ALS samples differed with regard to disease onset and duration. This is at least somehow offset by the advantage of using mRNA and miRNA analysis from the identical samples and a conservative set of significances. Further, the results of the current study are entirely based on bioinformatic prediction. However, the identification of miRNAs involved in neurodevelopment might be due to the fact that iPSC-derived neurons are still of fetal character. Nevertheless, miRNA-124 and miRNA-218 were also reported to be differentially regulated in adult mice and human tissues [41–43, 51], and similar two-headed expression are also reported for other developmental genes, e.g. neuronal transcriptional repressor (REST) [67, 68]. Therefore, more experimental studies including larger samples are required to further validate our findings.

In summary, we analyzed both miRNAs and mRNAs integrated profiles in the same subjects (SOD1 vs. TARDBP vs healthy controls) with an extensive and comprehensive bioinformatics approach to address the question on how much miRNA dysregulation might contribute to post-ranscriptional regulation of gene expression. In accordance with previously reported ALS studies [69, 70], we revealed a significant upregulation of MN-specific miRNAs in our cell lines (SOD1 mutant) and identified the commonly dysregulated pathways/networks of putative miRNAs, that may provide useful insights into the implicated molecular mechanisms of the disease. In our previous studies we have identified gene expression as a common pathomechanism in both, TARDBP-associated with RNA transcription and SOD1-connected to protein translation in hiPSC-derived MNs of ALS patients. Fitting to this, in the present study we found only significant miRNA-mRNA regulation enriched in SOD1-MNs, which was only significant in case of upregulated miRNA and downregulated targets. Of these miRNAs, four stood out if systemically comparing all five databases used, namely miRTarBase, TarBase, miRDB, TargetScan and miRWalk. The most frequent candidate mRNAs were CDK6, SLC6A1, and TGF-beta (beta1 and beta 2 isoforms). Thus, miRNA dysregulation might at least partly explain the finding of gene expression dysregulation at protein translation level in SOD1-MNs, but not TARDBP-MNs.

Materials and methods

Patient characteristics

We included patient cell lines carrying mutations in SOD1 (female, age at biopsy 46, D90A [one clone], male, age at biopsy 59, R115G [one clone]) and in TARDBP (a "benign" S393L, late onset primary anarthria with ALS/LMND, no clinical symptoms of FTD, female, age at biopsy 85, family history of ALS and PD and a "malign" G294V, early onset ALS, no clinical symptoms of FTD, male, age at biopsy 46, no family history, two clones from patient), which were identified by Sanger sequencing in clinical settings prior to fibroblast derivation and were compared to three different wildtype cell lines from healthy volunteers (female, age at biopsy 53; male, age at biopsy 60; and female, age at biopsy 45). An overview of the used cell lines is given in Table 1. All experiments were in accordance with the Helsinki convention and approved by the Ethical Committee of the Technische Universität Dresden (EK45022009, EK393122012) and patients and healthy volunteers gave their written consent prior to skin biopsy.

Generation of cell lines and differentiation into MNs

Fibroblast cell lines were established from skin biopsies obtained from familial ALS patients (two of each carrying SOD1 and TARDBP, respectively) which were compared to three different healthy control individuals (different families with different mutations; SOD1 hom. D90A, SOD1 het. R115G, TARDBP het. S393L and TARDBP het. G294V, respectively; different controls from different families, for details see also Table 1). In case of the control lines, genetic testing was performed and they were only included if this was negative for mutations in the four most frequent ALS genes *C9ORF72*, *SOD1*, *FUS* and *TARDBP*. The reprogramming procedure to obtain iPSC from fibroblasts and characterization of control iPSC lines was described previously [32, 71, 72].

The generation of human neural progenitor cells (NPC) and motor neurons (MN) was accomplished following the protocol from Reinhardt et al., Bursch et al. and Naumann *et al.* [71–73]. Importantly, the NPC culture was a resource for final MN differentiation, which was initiated by treatment with 1 μM purmorphamine (PMA) in N2B27 and supplemented with 1 μM retinoic acid (RA) on the third day. To increase the purity of MN enriched cell culture another split was performed on day 9 of the protocol. In parallel, the medium constitution was changed: Instead of PMA and RA, 10 ng/μl BDNF, 500 μM dbcAMP and 10 ng/μl GDNF was added to N2B27 ensuring neuronal maturation. All the iPSC lines

Table 1. Patient/proband characteristics.

Genotype	Sex	Age at Biopsy (Years)	Mutation	Family History	Age of Disease Onset	ALS Type	Clinical Characteristics	Disease Duration (Months)	Clones	DIV
Controls										
	Female	53	–	–	–	–		–	1	30
	Male	60	–	–	–	–		–	1	30
	Female	45	–	–	–	–		–	1	30
TDP43-ALS										
	Female	85	p.S393L	Pos. for ALS	85	Bulbar	Progressive anarthria, LMND, no clinical symptoms of FTD	48	1	30
	Male	46	p.G294V	neg for ALS	37	Spinal	Early onset ALS (37 years), monomelic right leg amyotrophy, no clinical symptoms of FTD	> 120 (alive)	2	30
SOD1-ALS										
	Male	59	p.R115G	Pos. for ALS (Mother and Brother)	n.d	Spinal	n.d	n.d	1	30
	Female	46	p.D90A	Pos. for ALS (Brother)	41	Spinal	Slowly progressive classical spinal ALS, no cognitive impairment	204	1	30

Patient/proband characteristics. Clinical characteristics of ALS participants and controls at the time of skin biopsies. Abbreviations: n.d, no data; LMND, lower motor neuron disease; DIV, days *in vitro*.

we used were low passage number (less than 20) and differentiated for 14–21 days of terminal differentiation (= total DIV 30). All these cell lines have been previously characterized including the acquisition of classical spinal motor neurons markers, electrophysiological function and the sequential appearance of progressive neurodegeneration [31, 32, 74]. In summary, immunolabeling detected the presence of neuronal (TuJ1 80%–90%, MAP2 80%–90%) and motor neuron specific markers (SMI32 70%–75%) in the cells without significant differences in neuron morphologies between wildtype controls ($n = 3$ subjects, 1 clone each) and ALS mutants (SOD1 $n = 2$ subjects, 1 clone each; TARDBP $n = 2$ subjects, 2 clones of one subject and 1 clone of second subject). There was no difference between wildtype and mutants SOD1 [31, 74] and TARDBP [32].

RNA extraction

After 30 DIV, each culture was washed by gently replacing the maturation medium with PBS warmed to 37°C. Total RNA (including miRNAs) from ~5×10^6 cells were extracted using the miRNeasy Mini Kit (Qiagen GmbH, Hilden, Germany) according to the manufacturer's protocol using the specific protocol for small amounts of RNA for the neuronal fraction including a column DNase digest for all samples. The RNA was eluted in Rnase-free water and RNA quality was assessed by measuring the ratio of absorbance at 260/280 nm using a Nanodrop 1000 Spectrometer (Thermo Scientific, USA) and RNA integrity was assessed using the Bioanalyzer 2100 (Agilent Technologies, Santa Clara, CA, USA). Each RNA sample was then divided into two aliquots that were applied either for the miRNA-Seq or mRNA-Seq.

RNA-Seq and bioinformatics analysis

The total RNA sequencing data were obtained from our previously published study [29]. All mRNA samples were sequenced using a HiSeq 2500 (Illumina, San Diego, CA, USA) 100 bp paired-end single lane run. We performed all bioinformatics analyses based on the human reference genome (hg38 (obtained from EnsEMBL assembly v100)) and comprehensive gene annotation. The total RNA-Seq data that support the findings of this study are openly available in the GEO database at GSE210969.

Small RNA-Seq and differential miRNA expression (DE-miRNA) analysis

Small RNA libraries were generated from total RNA extracted from iPSC-derived MNs (SOD1, TARDBP and healthy controls, 30 DIV) using TruSeq Small RNA Library Preparation Kit and sequenced on a Illumina Hiseq 2500 Sequencing system. An average of about 17 million fifty-nucleotide (50 base pairs) long single-end sequencing reads were produced for each sample. We mapped small RNA-Seq reads after trimming bases and quality control (QC) to the human genome using Bowtie algorithm (Bowtie 2.3.5.1) [75]. Prior to mapping, low quality reads were filtered out from subsequent analysis if they contained uncalled bases or if they were shorter than 18 bp after 3′ end quality clipping (Phred score < 10) and 3′ end trimming. The general pipeline for small

RNA-Seq analysis used in this study, including pre-alignment QA/QC, trim bases were performed using *Partek™ Flow™* software, v11.0. Post-alignment QA/QC, quantification, normalization, and differential gene expression analyses were performed in *Partek™ Genomics Suite™* software, v7.0. The processed aligned reads (BAM files) were then quantified against the miRBase 22 transcript annotations for mature miRNAs of the latest human genome assembly, hg38 (GRCh38) [76] using the Expectation Maximization (EM) algorithm, in which isoform expression levels are quantified across the whole genome at the same time [77]. Reads from miRNA genes were normalized using Reads Per Kilobase per Million mapped reads (RPKM) normalization method [78] for comparison between samples. The differential gene expression analysis was performed using one-way analysis of variance (ANOVA) model statistical approach with default parameters to analyze the difference between wildtype control and ALS mutant cell lines. To investigate the effect of ALS phenotypes and to generate significant DE-miRNAs among sample groups, we performed a linear contrast between mutant vs. control cell lines. In this comparison, a maximum filter of P-value ≤ 0.05 and a minimum absolute fold change $|\log2FC| \geq 1.5$ cut-off was applied.

Identification of target genes by inverse correlation and target prediction analysis

In order to identify list of specific genes that represent putative targets of DE-miRNAs, an *in silico* prediction analysis was performed using an integrated approach of validated and predicted miRNA-target interaction data obtained from five different databases. All databases have been searched for *homo sapiens*. Of these, two widely comprehensive and up-to-date databases miRTarBase v9.0 [79] and DIANA-TarBase v8.0 [80], contain validated miRNA targets and we retained all verified targets for which the miRNA-target interactions was classified as positive. In contrast, TargetScanHuman v8.0 (cumulative weighted context ++ scores < -0.1) [81], miRDB v6 (target score ≥ 70) [82], miRWalk v3 (predictions in 3′-UTR, 5′-UTR, and CDS, binding P-value ≥ 0.95) [83] consist of computationally predicted miRNA targets. To reduce the probability of false positive results and strengthen the results of interaction prediction, we performed an overlap of the targets that were identified by both experimentally validated and predicted miRNA-target interaction databases, and then by matching the DE-mRNAs selected from the GSE210969 dataset. The target genes of DE-miRNAs which were found overlapping with the DE-mRNAs were selected as the candidate target mRNAs/genes for further downstream analysis and extracted via the online tool Venny 2.1 (https://csbg.cnb.csic.es/BioinfoGP/venny.html) [84]. In particular, Venn diagram was used to visualize common miRNAs (62 DE-miRNAs) and common mRNAs (230 DE-mRNAs) obtained from five separate databases. This research was carried out within certain inclusion criteria: i) miRNAs found in all five databases were collected into a single list, ii) miRNAs from the common list that targeted at least three target genes were combined into a single list (Cutoff criteria, DE-miRNAs ≥ 3 DE-mRNAs) (Table 2). For integration analysis of DE-miRNA and gene expression data (DE-mRNA), Pearson and Spearman correlation coefficients and their P-values ($P \leq 0.05$) were calculated statistically significant (see below).

To identify negative correlations between miRNA and mRNA expression levels in ALS mutant vs controls, we performed Pearson and Spearman correlation analysis using miRNA-mRNA integrative approach of the *Partek™ Genomics Suite™* software, v7.0. This approach of correlating miRNA and mRNA expression data is useful to identify candidate miRNA target genes that are downregulated at the transcriptional level and are inversely correlated with the expression of the miRNA in the same corresponding samples. Briefly, normalized miRNA and mRNA read counts were sample-matched for all samples with both miRNA and mRNA sequencing data. The predicted target mRNAs of the particular miRNA were selected from both databases, considering experimentally validated and predicted interactions, and the resulting miRNA targets were further filtered to the genes that are differentially expressed in the MNs (mutant vs control) based on RNA-Seq analysis. Pearson and Spearman correlation coefficients and their P-values ≤ 0.05 (negative regulation) were calculated. Calculated correlation values between the upregulated miRNAs and their downregulated target genes from the miRNA profiling and RNA-Seq data revealed that several genes were targeted by a single miRNA in SOD1-ALS dataset. To address the functional significance of miRNA-mRNA interactions, the functional enrichment and network analysis of key genes were performed focusing on dysregulated mRNA targets for downregulated miRNAs in SOD1 mutant samples.

Functional annotation of target genes by GO and pathway analysis

To better interpret the possible pathways and target genes of the relevant miRNAs analysed in SOD1-ALS, gene ontology (GO) functions and pathway enrichment analyses of candidate genes were carried out by utilizing the EnrichR, an integrated online tool for gene list annotation and biological analysis [85]. GO analysis is a common method in functional enrichment analysis, aiming to provide biological attributes of the key genes such as biological processes (BP), molecular functions (MF), and cellular components (CC). Pathway analysis (Reactome and KEGG) is crucial in understanding different signaling and metabolic cascades and their associated molecular functions in a given biological system. The selected 23 overlapping target genes were imported and analyzed by EnrichR (http://amp.pharm.mssm.edu/Enrichr/) through its web interface [85]. The EnrichR tool calculates P-values using a Fisher's exact test and adjusts P-values using the Benjamini–Hochberg method to correct for multiple hypotheses testing. Pathway analysis in Reactome 2022 and KEGG 2021 Human was performed on the identified genes.

miRNA-target regulatory network

A miRNA-mRNA regulatory network was constructed containing the paired miRNA-mRNA expression profiles (selected from inclusion criteria, see above), and the putative target genes of DE-miRNAs were predicted. Furthermore, the key miRNAs and genes were identified based on a network topological property using NetworkAnalyzer v4.4.8 plugin of the Cytoscape software v.3.10.1 [86]. Top DE-miRNAs were selected for network generation because of their high degree of network connectivity within the network. In the miRNA-based network, miRNAs that were not annotated without a verified/predicted target in the above databases were excluded from further analysis. The network was analyzed and visualized with Cytoscape software v3.10.1 [86].

Statistical analysis

All statistical analyses including Hierarchical clustering (with Euclidean distance measure and average linkage clustering) and QC assessment were performed using *Partek™ Flow™* software, v11.0 and *Partek™ Genomics Suite™* software, v7.0. Differential miRNA expression was analyzed by applying a P-value filter (for attribute) of $P \leq 0.05$ to the one-way ANOVA results followed by false discovery rate (FDR) step-up for multiple

Table 2. Common miRNAs associated with SOD1-ALS (present study).

miRNA	Change in expression	Target genes
hsa-miR-124-3p	Upregulated	RARG, PAPSS2, CDK6, SLC16A1, PLEC, MTDH, STEAP3, TUBG1, TEX261, RAB11FIP1, KIAA0895, SFT2D2
hsa-miR-19b-3p	Upregulated	CNOT6, TRAK2, BNC2, CSPP1, FAT3, SAMD4A
has-miR-218	Upregulated	WAC, SLC6A1, RASEF
hsa-miR-145-5p	Upregulated	RTKN, TGFBR2, CDK6

Among the common 62 miRNAs, a set of four miRNAs (miR-124-3p, miR-19b-3p, miR-218 and miR-145-5p) were identified that regulated the expression of at least three target genes collected simultaneously from five distinct databases and these miRNAs may perform an important role in the regulation of post-transcriptional gene expression in SOD1-ALS.

comparisons. P-value ≤ 0.05 and log2FC ≥ 1.5 or log2FC ≤ -1.5 were considered as significant thresholds for the identification of differentially expressed genes. All of the gene expression samples presented in this study were designed for 3 biological replicates (mean ± standard error (SEM), $n \geq 3$) and the difference between sample groups for miRNAs target enrichment analysis were analyzed with Fisher's exact test using GraphPad Prism v9.4.1. A P-value ≤ 0.05 was considered to indicate a statistically significant difference. For the functional enrichment and regulatory network analysis, significantly enriched GO terms, pathways and modules were identified using a P-value ≤ 0.05 as the cut off value for statistical significance. RNA to miRNA correlation analysis was performed using *Partek™ Genomics Suite™* software, v7.0. The Pearson and Spearman correlation coefficients and their P-values (P-value ≤ 0.05) were calculated between DE-miRNAs and DE-mRNAs.

Acknowledgements

We acknowledge the great help of Jared Sterneckert for sharing SOD1 and control iPSC cell lines. We are also grateful to Christoph Dieterich for sharing RNA-Seq data of our cell lines with us. The authors acknowledge BioRender for providing the copyright permission of publicly available illustrations that have been used to create Fig. 1 and graphical abstract.

Author contributions

A.H. and B.P.D. conceived the project and outlined the study. B.P.D. and A.F. performed the methodology. B.P.D. carried out the software, validation, formal analysis and data curation, wrote the original draft and investigated the data. A.H., A.F., and J.H.W. reviewed, and edited the manuscript, and supervised the data. A.H. administrated the project and carried out the funding acquisition. All authors have read and agreed to the published version of the manuscript.

Supplementary data

Supplementary data is available at *HMG Journal* online.

Conflict of interest statement: The authors declare that they have no competing interests related to the direct applications of this research.

Funding

A.H. is supported by the Hermann and Lilly Schilling-Stiftung für medizinische Forschung im Stifterverband. Part of the work (author B.P.D.) was funded by the framework of the Professorinnenprogramm III (University of Rostock) of the German federal and state governments.

Data availability

All of the raw (fastq files) and normalized small RNA-Seq expression data generated in this study have been deposited in the NCBI Gene Expression Omnibus (GEO), with the accession number as GSE210969.

References

1. Goutman SA, Hardiman O, Al-Chalabi A. *et al.* Emerging insights into the complex genetics and pathophysiology of amyotrophic lateral sclerosis. *Lancet Neurol* 2022;**21**:465–479.
2. Renton AE, Chiò A, Traynor BJ. State of play in amyotrophic lateral sclerosis genetics. *Nat Neurosci* 2014;**17**:17–23.
3. Zou ZY, Zhou ZR, Che CH. *et al.* Genetic epidemiology of amyotrophic lateral sclerosis: a systematic review and meta-analysis. *J Neurol Neurosurg Psychiatry* 2017;**88**:540–549.
4. Saez-Atienzar S, Bandres-Ciga S, Langston RG. *et al.* Genetic analysis of amyotrophic lateral sclerosis identifies contributing pathways and cell types. *Sci Adv* 2021;**7**:eabd9036.
5. Taylor JP, Brown RH Jr, Cleveland DW. Decoding ALS: from genes to mechanism. *Nature* 2016;**539**:197–206.
6. Keller BA, Volkening K, Droppelmann CA. *et al.* Co-aggregation of RNA binding proteins in ALS spinal motor neurons: evidence of a common pathogenic mechanism. *Acta Neuropathol* 2012;**124**:733–747.
7. Bunton-Stasyshyn RK, Saccon RA, Fratta P. *et al.* SOD1 function and its implications for amyotrophic lateral sclerosis pathology: new and renascent themes. *Neuroscientist* 2015;**21**:519–529.
8. Butti Z, Patten SA. RNA dysregulation in amyotrophic lateral sclerosis. *Front Genet* 2018;**9**:712.
9. Pham J, Keon M, Brennan S. *et al.* Connecting RNA-modifying similarities of TDP-43, FUS, and SOD1 with MicroRNA dysregulation amidst a renewed network perspective of amyotrophic lateral sclerosis proteinopathy. *Int J Mol Sci* 2020;**21**:3464.
10. Bartel DP. MicroRNAs: genomics, biogenesis, mechanism, and function. *Cell* 2004;**116**:281–297.
11. Friedman RC, Farh KK, Burge CB. *et al.* Most mammalian mRNAs are conserved targets of microRNAs. *Genome Res* 2009;**19**:92–105.
12. Lagos-Quintana M, Rauhut R, Lendeckel W. *et al.* Identification of novel genes coding for small expressed RNAs. *Science* 2001;**294**:853–858.
13. Selbach M, Schwanhäusser B, Thierfelder N. *et al.* Widespread changes in protein synthesis induced by microRNAs. *Nature* 2008;**455**:58–63.
14. Fabian MR, Sonenberg N, Filipowicz W. Regulation of mRNA translation and stability by microRNAs. *Annu Rev Biochem* 2010;**79**:351–379.

15. Lewis BP, Shih IH, Jones-Rhoades MW. *et al.* Prediction of mammalian microRNA targets. *Cell* 2003;**115**:787–798.
16. Lim LP, Lau NC, Garrett-Engele P. *et al.* Microarray analysis shows that some microRNAs downregulate large numbers of target mRNAs. *Nature* 2005;**433**:769–773.
17. Paez-Colasante X, Figueroa-Romero C, Sakowski SA. *et al.* Amyotrophic lateral sclerosis: mechanisms and therapeutics in the epigenomic era. *Nat Rev Neurol* 2015;**11**:266–279.
18. Emde A, Eitan C, Liou LL. *et al.* Dysregulated miRNA biogenesis downstream of cellular stress and ALS-causing mutations: a new mechanism for ALS. *EMBO J* 2015;**34**:2633–2651.
19. Campos-Melo D, Droppelmann CA, He Z. *et al.* Altered microRNA expression profile in amyotrophic lateral sclerosis: a role in the regulation of NFL mRNA levels. *Mol Brain* 2013;**6**:26.
20. Figueroa-Romero C, Hur J, Lunn JS. *et al.* Expression of microRNAs in human post-mortem amyotrophic lateral sclerosis spinal cords provides insight into disease mechanisms. *Mol Cell Neurosci* 2016;**71**:34–45.
21. Rinchetti P, Rizzuti M, Faravelli I. *et al.* MicroRNA metabolism and dysregulation in amyotrophic lateral sclerosis. *Mol Neurobiol* 2018;**55**:2617–2630.
22. Cloutier F, Marrero A, O'Connell C. *et al.* MicroRNAs as potential circulating biomarkers for amyotrophic lateral sclerosis. *J Mol Neurosci* 2015;**56**:102–112.
23. Peters OM, Ghasemi M, Brown RH Jr. Emerging mechanisms of molecular pathology in ALS. *J Clin Invest* 2015;**125**:1767–1779.
24. Rotem N, Magen I, Ionescu A. *et al.* ALS along the axons—expression of coding and noncoding RNA differs in axons of ALS models. *Sci Rep* 2017;**7**:44500.
25. De Santis R, Santini L, Colantoni A. *et al.* FUS mutant human motoneurons display altered transcriptome and microRNA pathways with implications for ALS pathogenesis. *Stem Cell Reports* 2017;**9**:1450–1462.
26. Capauto D, Colantoni A, Lu L. *et al.* A regulatory circuitry between Gria2, miR-409, and miR-495 is affected by ALS FUS mutation in ESC-derived motor neurons. *Mol Neurobiol* 2018;**55**:7635–7651.
27. Liguori M, Nuzziello N, Introna A. *et al.* Dysregulation of MicroRNAs and target genes networks in peripheral blood of patients with sporadic amyotrophic lateral sclerosis. *Front Mol Neurosci* 2018;**11**:288.
28. Dash BP, Hermann A. Combination of novel RNA sequencing and sophisticated network modeling to reveal a common denominator in amyotrophic lateral sclerosis? *Neural Regen Res* 2023;**18**:2403–2405.
29. Dash BP, Freischmidt A, Weishaupt JH. *et al.* Downstream effects of mutations in SOD1 and TARDBP converge on gene expression impairment in patient-derived motor neurons. *Int J Mol Sci* 2022;**23**:9652.
30. Dash BP, Naumann M, Sterneckert J. *et al.* Genome wide analysis points towards subtype-specific diseases in different genetic forms of amyotrophic lateral sclerosis. *Int J Mol Sci* 2020;**21**:6938.
31. Günther R, Pal A, Williams C. *et al.* Alteration of mitochondrial integrity as upstream event in the pathophysiology of SOD1-ALS. *Cells* 2022;**11**:1246.
32. Kreiter N, Pal A, Lojewski X. *et al.* Age-dependent neurodegeneration and organelle transport deficiencies in mutant TDP43 patient-derived neurons are independent of TDP43 aggregation. *Neurobiol Dis* 2018;**115**:167–181.
33. Stappert L, Roese-Koerner B, Brüstle O. The role of microRNAs in human neural stem cells, neuronal differentiation and subtype specification. *Cell Tissue Res* 2015;**359**:47–64.
34. Cai Y, Yu X, Hu S. *et al.* A brief review on the mechanisms of miRNA regulation. *Genomics Proteomics Bioinformatics* 2009;**7**:147–154.
35. Kovanda A, Leonardis L, Zidar J. *et al.* Differential expression of microRNAs and other small RNAs in muscle tissue of patients with ALS and healthy age-matched controls. *Sci Rep* 2018;**8**:5609.
36. Liu H, Lan S, Shi XJ. *et al.* Systematic review and meta-analysis on microRNAs in amyotrophic lateral sclerosis. *Brain Res Bull* 2023;**194**:82–89.
37. De Felice B, Annunziata A, Fiorentino G. *et al.* miR-338-3p is overexpressed in blood, CFS, serum and spinal cord from sporadic amyotrophic lateral sclerosis patients. *Neurogenetics* 2014;**15**:243–253.
38. Wakabayashi K, Mori F, Kakita A. *et al.* Analysis of microRNA from archived formalin-fixed paraffin-embedded specimens of amyotrophic lateral sclerosis. *Acta Neuropathol Commun* 2014;**2**:173.
39. Rizzuti M, Filosa G, Melzi V. *et al.* MicroRNA expression analysis identifies a subset of downregulated miRNAs in ALS motor neuron progenitors. *Sci Rep* 2018;**8**:10105.
40. Chen H, Qian K, Du Z. *et al.* Modeling ALS with iPSCs reveals that mutant SOD1 misregulates neurofilament balance in motor neurons. *Cell Stem Cell* 2014;**14**:796–809.
41. Vaz AR, Vizinha D, Morais H. *et al.* Overexpression of miR-124 in motor neurons plays a key role in ALS pathological processes. *Int J Mol Sci* 2021;**22**:6128.
42. Amin ND, Senturk G, Costaguta G. *et al.* A hidden threshold in motor neuron gene networks revealed by modulation of miR-218 dose. *Neuron* 2021;**109**:3252–3267.e6.
43. Gentile G, Morello G, La Cognata V. *et al.* Dysregulated miRNAs as biomarkers and Therapeutical targets in neurodegenerative diseases. *J Pers Med* 2022;**12**:770.
44. Sun Y, Luo ZM, Guo XM. *et al.* An updated role of microRNA-124 in central nervous system disorders: a review. *Front Cell Neurosci* 2015;**9**:193.
45. Neo WH, Yap K, Lee SH. *et al.* MicroRNA miR-124 controls the choice between neuronal and astrocyte differentiation by fine-tuning Ezh2 expression. *J Biol Chem* 2014;**289**:20788–20801.
46. Hou Q, Ruan H, Gilbert J. *et al.* MicroRNA miR124 is required for the expression of homeostatic synaptic plasticity. *Nat Commun* 2015;**6**:10045.
47. Cunha C, Santos C, Gomes C. *et al.* Downregulated glia interplay and increased miRNA-155 as promising markers to track ALS at an early stage. *Mol Neurobiol* 2018;**55**:4207–4224.
48. Zhou F, Zhang C, Guan Y. *et al.* Screening the expression characteristics of several miRNAs in G93A-SOD1 transgenic mouse: altered expression of miRNA-124 is associated with astrocyte differentiation by targeting Sox2 and Sox9. *J Neurochem* 2018;**145**:51–67.
49. Marcuzzo S, Bonanno S, Kapetis D. *et al.* Up-regulation of neural and cell cycle-related microRNAs in brain of amyotrophic lateral sclerosis mice at late disease stage. *Mol Brain* 2015;**8**:5.
50. Ghafouri-Fard S, Shoorei H, Bahroudi Z. *et al.* An update on the role of miR-124 in the pathogenesis of human disorders. *Biomed Pharmacother* 2021;**135**:111198.
51. Foggin S, Mesquita-Ribeiro R, Dajas-Bailador F. *et al.* Biological significance of microRNA biomarkers in ALS-innocent bystanders or disease culprits? *Front Neurol* 2019;**10**:578.
52. Waller R, Wyles M, Heath PR. *et al.* Small RNA sequencing of sporadic amyotrophic lateral sclerosis cerebrospinal fluid reveals differentially expressed miRNAs related to neural and glial activity. *Front Neurosci* 2017;**11**:731.

53. Vrabec K, Boštjančič E, Koritnik B. *et al.* Differential expression of several miRNAs and the host genes AATK and DNM2 in leukocytes of sporadic ALS patients. *Front Mol Neurosci* 2018;**11**:106.
54. Chen Y, Wei Q, Chen X. *et al.* Aberration of miRNAs expression in leukocytes from sporadic amyotrophic lateral sclerosis. *Front Mol Neurosci* 2016;**9**:69.
55. Yelick J, Men Y, Jin S. *et al.* Elevated exosomal secretion of miR-124-3p from spinal neurons positively associates with disease severity in ALS. *Exp Neurol* 2020;**333**:113414.
56. Ranganathan S, Bowser R. p53 and cell cycle proteins participate in spinal motor neuron cell death in ALS. *Open Pathol J* 2010;**4**: 11–22.
57. Cheng LC, Pastrana E, Tavazoie M. *et al.* miR-124 regulates adult neurogenesis in the subventricular zone stem cell niche. *Nat Neurosci* 2009;**12**:399–408.
58. Silber J, Lim DA, Petritsch C. *et al.* miR-124 and miR-137 inhibit proliferation of glioblastoma multiforme cells and induce differentiation of brain tumor stem cells. *BMC Med* 2008;**6**:14.
59. Hoye ML, Koval ED, Wegener AJ. *et al.* MicroRNA profiling reveals marker of motor neuron disease in ALS models. *J Neurosci* 2017;**37**:5574–5586.
60. Thiebes KP, Nam H, Cambronne XA. *et al.* miR-218 is essential to establish motor neuron fate as a downstream effector of Isl1-Lhx3. *Nat Commun* 2015;**6**:7718.
61. Galbiati M, Crippa V, Rusmini P. *et al.* Multiple roles of transforming growth factor Beta in amyotrophic lateral sclerosis. *Int J Mol Sci* 2020;**21**:4291.
62. Wong CO, Venkatachalam K. Motor neurons from ALS patients with mutations in C9ORF72 and SOD1 exhibit distinct transcriptional landscapes. *Hum Mol Genet* 2019;**28**:2799–2810.
63. Oppenheim RW, Prevette D, Haverkamp LJ. *et al.* Biological studies of a putative avian muscle-derived neurotrophic factor that prevents naturally occurring motoneuron death in vivo. *J Neurobiol* 1993;**24**:1065–1079.
64. Duque T, Gromicho M, Pronto-Laborinho AC. *et al.* Transforming growth factor-β plasma levels and its role in amyotrophic lateral sclerosis. *Med Hypotheses* 2020;**139**:109632.
65. Meroni M, Crippa V, Cristofani R. *et al.* Transforming growth factor beta 1 signaling is altered in the spinal cord and muscle of amyotrophic lateral sclerosis mice and patients. *Neurobiol Aging* 2019;**82**:48–59.
66. D'Arrigo A, Colavito D, Peña-Altamira E. *et al.* Transcriptional profiling in the lumbar spinal cord of a mouse model of amyotrophic lateral sclerosis: a role for wild-type superoxide dismutase 1 in sporadic disease? *J Mol Neurosci* 2010;**41**:404–415.
67. Lu T, Aron L, Zullo J. *et al.* REST and stress resistance in ageing and Alzheimer's disease. *Nature* 2014;**507**:448–454.
68. Nechiporuk T, McGann J, Mullendorff K. *et al.* The REST remodeling complex protects genomic integrity during embryonic neurogenesis. *elife* 2016;**5**:e09584.
69. Ricci C, Marzocchi C, Battistini S. MicroRNAs as biomarkers in amyotrophic lateral sclerosis. *Cells* 2018;**7**:219.
70. Joilin G, Leigh PN, Newbury SF. *et al.* An overview of MicroRNAs as biomarkers of ALS. *Front Neurol* 2019;**10**:186.
71. Bursch F, Kalmbach N, Naujock M. *et al.* Altered calcium dynamics and glutamate receptor properties in iPSC-derived motor neurons from ALS patients with C9orf72, FUS, SOD1 or TDP43 mutations. *Hum Mol Genet* 2019;**28**:2835–2850.
72. Naumann M, Pal A, Goswami A. *et al.* Impaired DNA damage response signaling by FUS-NLS mutations leads to neurodegeneration and FUS aggregate formation. *Nat Commun* 2018;**9**:335.
73. Reinhardt P, Glatza M, Hemmer K. *et al.* Derivation and expansion using only small molecules of human neural progenitors for neurodegenerative disease modeling. *PLoS One* 2013;**8**:e59252.
74. Naujock M, Stanslowsky N, Bufler S. *et al.* 4-Aminopyridine induced activity rescues Hypoexcitable motor neurons from amyotrophic lateral sclerosis patient-derived induced pluripotent stem cells. *Stem Cells* 2016;**34**:1563–1575.
75. Langmead B, Salzberg SL. Fast gapped-read alignment with bowtie 2. *Nat Methods* 2012;**9**:357–359.
76. Kozomara A, Birgaoanu M, Griffiths-Jones S. miRBase: from microRNA sequences to function. *Nucleic Acids Res* 2019; **47**:D155–d162.
77. Xing Y, Yu T, Wu YN. *et al.* An expectation-maximization algorithm for probabilistic reconstructions of full-length isoforms from splice graphs. *Nucleic Acids Res* 2006;**34**:3150–3160.
78. Mortazavi A, Williams BA, McCue K. *et al.* Mapping and quantifying mammalian transcriptomes by RNA-Seq. *Nat Methods* 2008;**5**: 621–628.
79. Huang HY, Lin YC, Cui S. *et al.* miRTarBase update 2022: an informative resource for experimentally validated miRNA-target interactions. *Nucleic Acids Res* 2022;**50**:D222–d230.
80. Karagkouni D, Paraskevopoulou MD, Chatzopoulos S. *et al.* DIANA-TarBase v8: a decade-long collection of experimentally supported miRNA-gene interactions. *Nucleic Acids Res* 2018;**46**:D239–d245.
81. McGeary SE, Lin KS, Shi CY. *et al.* The biochemical basis of microRNA targeting efficacy. *Science* 2019;**366**:eaav1741.
82. Chen Y, Wang X. miRDB: an online database for prediction of functional microRNA targets. *Nucleic Acids Res* 2020;**48**: D127–d131.
83. Sticht C, De La Torre C, Parveen A. *et al.* miRWalk: an online resource for prediction of microRNA binding sites. *PLoS One* 2018;**13**:e0206239.
84. Oliveros, JC. (2007-2015) Venny. An Interactive Tool for Comparing Lists With Venn's Diagrams. https://bioinfogp.cnb.csic.es/tools/venny/index.html.
85. Kuleshov MV, Jones MR, Rouillard AD. *et al.* Enrichr: a comprehensive gene set enrichment analysis web server 2016 update. *Nucleic Acids Res* 2016;**44**:W90–W97.
86. Shannon P, Markiel A, Ozier O. *et al.* Cytoscape: a software environment for integrated models of biomolecular interaction networks. *Genome Res* 2003;**13**:2498–2504.